

## Article

# Application of Cold Region Regenerable Biomass in Phosphorus Adsorption in Reclaimed Water

Jinghui Wu <sup>1</sup>, Xiangyu Li <sup>2</sup>, Zhian Ying <sup>3</sup>, Chi Wang <sup>3</sup>, Wu Yang <sup>3</sup>, Mingxin Huo <sup>3</sup>, Chyi-How Lay <sup>4</sup> and Xianze Wang <sup>3,\*</sup>

<sup>1</sup> School of Municipal and Environmental Engineering, Jilin Jianzhu University, Changchun 130118, China

<sup>2</sup> Flemish Institute for Technological Research (VITO), Mol 2400, Belgium

<sup>3</sup> School of Environment, Northeast Normal University, Changchun 130117, China

<sup>4</sup> General Education Center, Feng Chia University, Taichung 40724, Taiwan

\* Correspondence: wangxz940@nenu.edu.cn; Tel.: +86-181-4308-2239

Received: 15 August 2019; Accepted: 29 August 2019; Published: 31 August 2019



**Abstract:** In order to enhance the using efficiency of the adsorbent and decrease production costs, reclaimed saturation Lanthanum modified pine needles (LH pine needles) have been studied as a possible solution. Pine needles gathered from the woods of Northeast China area were used as raw material for generating LH pine needles by alkali-isopropanol treatment and chemical precipitation. To explore the utilization of LH pine needles as a recycling adsorbent in wastewater treatment plants (WWTPs) and laboratory water distribution. Results show that removal effective of phosphorus (P) by LH pine needles in low concentration reclaimed water of WWTPs was 41% and up to more than 92% in its adding standard. In the wide pH range, LH pine has an effective adsorption capacity for phosphorus; pH can also interfere with the adsorption capacity of LH pine as there is a negative correlation between them. The adsorption of phosphorus by LH pine needles is divided into three stages with a pH ranging from 3–11. Ligand exchange reaction, electrostatic reaction and Lewis acid reaction are  $\text{PO}_4^{3-}$  adsorption mechanism. The analysis of the recycling efficiency of LH pine needles proved that LH pine needles have good regeneration performance. After being eluted by NaOH regeneration agent for more than 10 times, the adsorption efficiency of phosphorus can still be stable at over 90% in seven cycles.

**Keywords:** reclaimed water; adsorption mechanism; regenerable; biomass adsorbent; adsorbent

## 1. Introduction

As early as 2015, the United Nations Environment Programme addressed that waste water was an undervalued resource that should not be wasted, while reclaimed water had most added value [1,2]. Utilization of reclaimed water is receiving increased attention in many regions, countries and different industries around the world, such as the United States, Europe, Singapore and China [3–5]. In China, the applications of reclaimed water include groundwater recharge, supply for rivers and lakes, landscapes, irrigation of agricultural crops and industrial reuse, the mainstream of sewage is still discharged [2–5]. Due to the complexity of sewage and the limitation of treatment process, the regenerated water after deep treatment still contains plant nutrients such as nitrogen and phosphorus (P). Although reclaimed water of waste water treatment plants (WWTPs) contains low concentrations of pollutants, it may still threaten the environment by normal pollutant which supplied directly [6]. Phosphorus (P), a necessity of life while polluting the ecological environment in many ways, is also an important contaminant in reclaimed water that should be removed.

P removal mechanisms in WWTPs include physical (sedimentation), chemical (adsorption, precipitation and complexation) and biological processes (vegetation and microbial) [7,8], as well as

the emission of phosphine gas [9]. Due to different P concentrations in solutions, the P adsorption capacities of substrates vary greatly [10].

Our previous research of the removal of P was only at laboratory scale of water distribution, while research and mechanism analysis in actual WWTPs were yet executed [11]. Adsorption mechanism is a necessary part of adsorbent which plays an important role in pollutant removal of reclaimed water. During the last decade, studies of adsorbent on phosphorus have been conducted varied, including in sodium bentonite/clay (BC) [12], Modified cottonwood fiber, etc. [13]. The effectiveness for P removal with different absorbing materials have also been compared [11,14,15]. However, most adsorbent studied to date are used to treat P of sewage in few cycles, and very few studies investigated the use of adsorbent in recycling, let alone use a recycling biosorbent.

Different kinds of natural and synthetic adsorbents have been used to remove pollutants from wastewater [16,17]. Biomass adsorbent has been widely used in wastewater treatment due to its purification effect on lower phosphorus wastewater. 2.12 million hectares of camphor pine and red pine in Changbai Mountain in the northeast of China produces 14.84 million tons of pine needles annually. However, these pine needles are abandoned normally. Biomass adsorbent can improve the adsorption efficiency by changing the adsorption properties: increasing the pore channel and specific surface area of adsorbent, or changing the cationic species attached to the surface of adsorbent. Hence, pine needles with pore structure are supposed to be good carbon-based biomass adsorbents. Thus, it is widely used in wastewater treatment [18]. The modification methods of the adsorbents studied at present mainly include biological modification [19–21], physical modification [22] and chemical modification [23]. Based on the chemical modification method, the properties of biomass can be easily changed using metal hydroxides (oxides). Lanthanum hydroxide (lanthanum oxide) is an environmentally friendly substance [24], and has proven to have a very high phosphorus adsorption and removal efficiency [25–27].

At present, there is no engineering study on the application of LH pine needles made by loading lanthanum hydroxide on pine needles in reclaimed water. Based on this, the waste pine needles were utilized as resources, and the improvement conditions of the properties of modified biomass adsorbent were comprehensively considered, which solved the problem of disposal of waste resources and saved the use cost of Regenerable Biomass Adsorbent. Additionally, we attempted to identify the influencing factors involved in P removal by mechanism analysis. Phosphorus removal in reclaimed water by the Regenerable Biomass Adsorbent must be a key element of this study.

## 2. Materials and Methods

### 2.1. Chemicals

All chemicals used for this study were analytical grade, purchased from Tianjin Fuchen Chemical. All solutions were prepared with distilled water. Lanthanum nitrate hexhydrate ( $\text{La}(\text{NO}_3)_3 \cdot 6\text{H}_2\text{O}$ ) was used to prepare the adsorbent LH pine needles. Phosphorus stock solutions were prepared using potassium dihydrogen phosphorus ( $\text{KH}_2\text{PO}_4$ ).

### 2.2. Preparation of LH and AI Pine Needles

LH and AI (alkali-isopropanol) pine needles were synthesized by the following procedures:

Pine needles were gathered from the woods behind Northeast Normal University (NENU). As displayed in Figure 1, we received full permission from Northeast Normal University for collecting the pine needles from the woods that belongs to NENU, and the geographic coordinates are 125.43° E, 43.83° N. These pine needles were washed five times with distilled water to remove dust. The samples were then dried overnight at a temperature of 353 K. The needle samples were then crushed to a size of approximately 1–2.5 mm in length, and then soaked in a mixture of 3 M sodium hydroxide (NaOH) and isopropanol (V NaOH/V isopropanol = 1:1) for 24 h. The soaked pine needles were then washed again with distilled water and dried overnight, again at a temperature of 353 K. The cooled

AI pine needles were then set aside for further use. take 20 g AI pine needles added to 250 mL of 0.1 M  $\text{La}(\text{NO}_3)_3$  after, stirred for 1 h, and deposited for 5 h. An ammonia solution (28%, wt%) was then added drop by drop to adjust the pH within the range of 8–9. The samples were again deposited for 10 h, washed five times with distilled water, and dried at 353 K for 720 min. The synthesized procedures used in this research are the same as in our previous study [11].

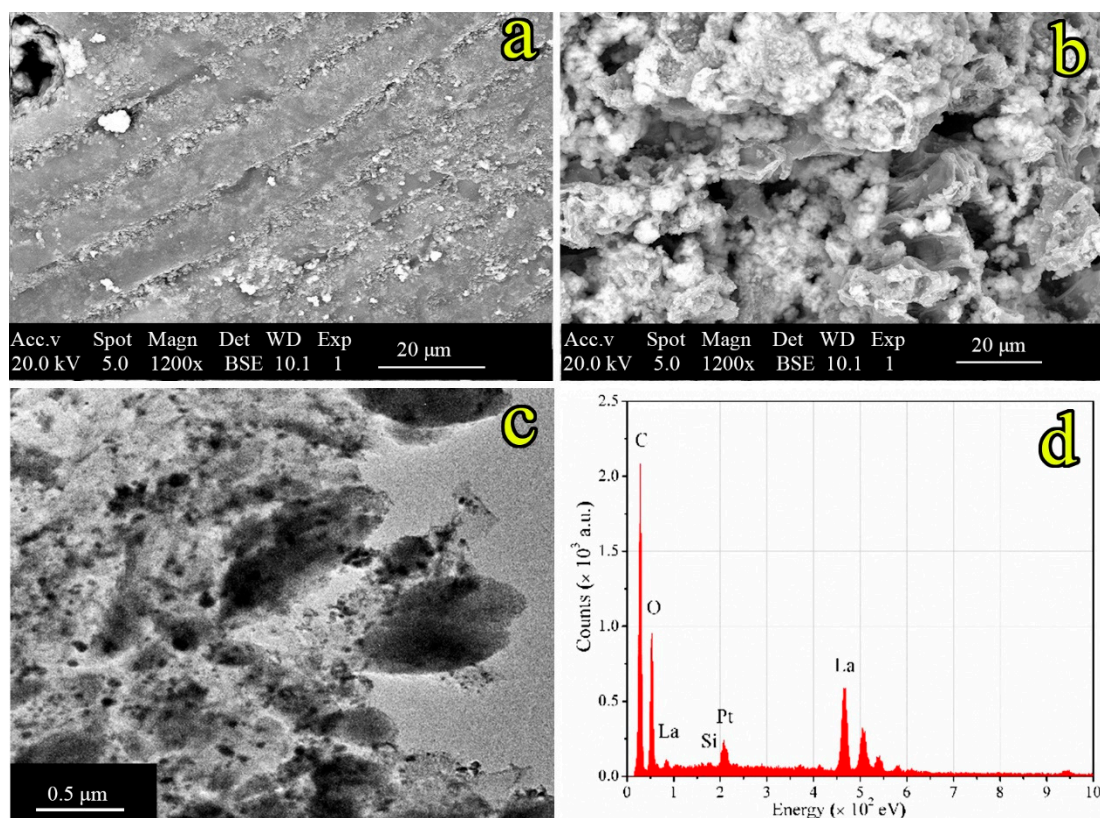


**Figure 1.** SEM chart of outer surface of LH pine needles (a), SEM chart of interior structure of AI pine needles (b), TEM chart of LH pine needles (c) and EDAX of LH pine needles (d).

### 2.3. Batch Adsorption Experiments

Batch experiments were conducted to investigate the phosphorus adsorption performances of LH pine needles. Samples were placed into multiple 150 mL glass stoppered conical flasks containing 100 mL phosphorus solutions at target concentrations. Flasks were then placed on a rotary shaker and stirred at 160 rpm at a temperature of 298 K. Samples of 0.1 g LH pine needles were added to a series of solutions (reclaimed water from west-north-south suburb WWTPs) with standard addition of phosphorus concentrations (10 mg/L) for 720 min at a temperature of 298 K. The effect of initial pH was studied by mixing 0.1 g LH pine needles with 10 mg/L phosphorus solution at pH values ranging from 3 to 10 for 720 min. Solution pH was adjusted with 0.1 mol/L HCl and NaOH.

The experiments of the recycling efficiency of LH pine needles were then conducted. The adsorption saturated LH pine needles were filtered by 0.45 μm glass fiber membrane and then added to 100 mL regenerative solvent (ammonia, NaCl, and NaOH) with a concentration of 0.1 mol/L. After further centrifugation for 30 min, the analytical LH pine needle was filtered through a vacuum extraction filter. The solution containing phosphate was determined by ion chromatography. The regenerated LH pine needles were washed 3 times with deionized water, and the adsorption and desorption experiments were conducted once again.

All of the experiments were carried out in triplicate.

## 2.4. Analytical Methods

Phosphorus concentrations were determined using a Metrohm 881 ion chromatograph coupled with a Metrosep A Supp 4 column. A solution with 1.8 mm of Na<sub>2</sub>CO<sub>3</sub> and 1.7 mm of NaHCO<sub>3</sub> was used as a mobile phase with a flow rate of 1.2 mL/min.

The concentration of residual lanthanum ions in the solutions after the adsorption process was determined. Phosphorus adsorption capacities ( $q_e$ , mg P/g) and removal efficiencies (%) were determined using the following equations:

$$q_e = \frac{V \times (C_0 - C_e)}{1000 \times m} \quad (1)$$

$$\text{Removal efficiency (\%)} = \left(1 - \frac{C_e}{C_0}\right) \times 100\% \quad (2)$$

In these equations,  $q_e$  (mg P/g) was the phosphorus adsorption capacity,  $V$  (mL) was the volume of the solution,  $C_0$  and  $C_e$  (mg/L) were respectively the concentrations before and after adsorption and  $m$  (g) was the adsorbent mass.

## 3. Results and Discussion

### 3.1. Characteristics of LH Pine Needles

The Fourier transform infrared spectra of AI pine needles and LH pine needles were obtained by Thermo Fisher Nicolet 6700 spectrometer. The sample was prepared by KBr tablet. The test range was 450 cm<sup>-1</sup>~4000 cm<sup>-1</sup>. The morphological structures of AI pine needles and LH pine needles were obtained by SEM (XL30-ESEM, FEI, Portland, OR, USA) and TEM (TECNAIF20, FEI, Portland, OR State, USA).

#### (1) Surface morphology analysis

As shown in Figure 1, SEM images and TEM images of LH pine needles are shown. It can be seen from Figure 1a that the LH pine needle have many pleated outer surfaces, but the appearance is smooth without significant change, indicating that the hydroxide and isopropanol pretreatment does not destroy the lignified skin of the outer surface of the pine needle. However, significant changes can be seen on the inside as shown in Figure 1b, and many fine white spots can be seen by observing the inside of the LH pine needle, these spots being confirmed as lanthanum oxide according to the EDAX pattern, 11.84% (wt%) of La was obviously loaded on the pine needle. pretreatment destroyed the hydrogen bond between lignin and carbohydrate or cellulose molecules, and the organic matter of pine needle tissue was extracted to make its structure fluffy and form porous structure. The exposure of the fibers contributes to a greater specific surface area, making the attachment to lanthanum ions easier and providing a greater surface area and surface active functionality.

The presence of black particles can also be observed from TEM Figure 1c of the LH pine needles, and the disordered mosaic of particles of varying sizes in the pores resulting from the uneven distribution of wrinkles. It was further proved that La modified pine needles.

#### (2) X-ray diffraction analysis

As shown in Figure 2 are X-ray diffraction (XRD) patterns of LH pine needles, the diffraction peak shape of XRD has a great relation to whether the sample is crystalline or amorphous: if the peak shape is a steamed bread peak, it is a standard amorphous; if the peak shape is a sharp peak, it is a crystal. The sharper the peak, the smaller the half height width, the smaller the grain size, the higher the crystallinity [28]. It can be seen that the diffraction peaks of La match well with the cubic structure of La (JCPDS NO.83-1345) in the fixed figure. The results showed that LH pine needle were successfully prepared. Moreover, the characteristics of the amorphous solids of the pine needles were not changed

after the pine needles were loaded with the metals La, indicating the structural stability of the modified pine needles [29].

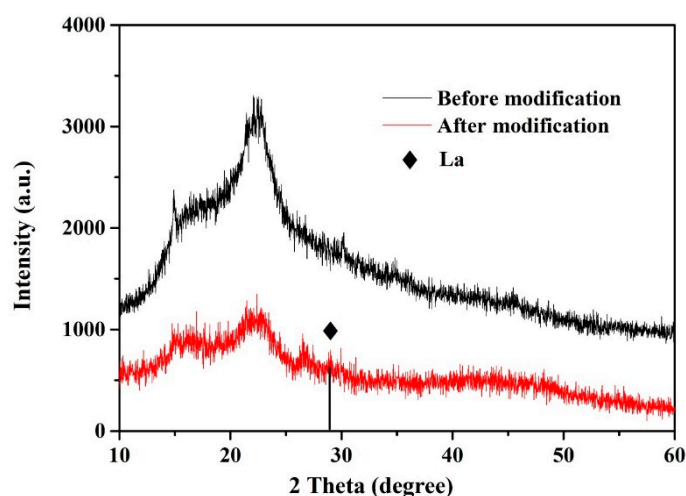


Figure 2. X-ray diffraction spectrogram of LH pine needle.

### 3.2. Adsorption of Phosphorus in Reclaimed Water with LH Pine Needles as Recycling Adsorbent

In the actual wastewater adsorption experiment, the original water from the secondary effluent of the treated sewage plant was extracted by adding standard, and the recovery rate was above 80%. Reclaimed water was selected from typical WWTPs in Changchun. The different treatment processes (Anaerobic-Anoxic-Oxic ( $A_2/O$ ) and Anoxic Oxic ( $A/O$ )) of three WWTPs were selected, providing 81.2% of the entire city in daily processing capacity. Therefore, the study of reclaimed water has practical research value (Tables 1 and 2).

**Table 1.** Basic situation of typical sewage treatment plants in Changchun City. WWTP: waste water treatment plant.

Provincial	City	Site	Treatment Process	Build-Up Time (mm/year)	Design Disposal Capability (t/day)	Actual Capacity (t/day)
Jilin	Changchun	Southern suburb WWTP	$A_2/O$	08/2009	15.00	7.55
Jilin	Changchun	Northern suburb WWTP	$A_2/O$	08/2007	39.00	33.84
Jilin	Changchun	Western suburb WWTP	$A/O$	08/2002	15.00	7.25

**Table 2.** Maximum total phosphorus concentration emission allowance in GB18918-2002 (average daily value, mg/L).

Basic Control Item	Standard A of the First Class	Standard B of the First Class	Standard of the Second Class	Standard of the Third Class
Total phosphorus (by P)				
before the construction in 31 December 2015	1	1.5	3	5
after the construction in 1 January 2016	0.5	1	3	5

The adsorption of phosphorus for reclaimed water with standard addition by LH pine needles followed. The content of the actual water body composition is very complex, and there were a lot of coexisting pollutants that were both organic and inorganic; the ionic strength and pH would have a great influence on the adsorption process of LH pine needles. Therefore, in the experiment process, the water of the typical wastewater treatment plant in Changchun was selected as the base water to determine the phosphorus adsorption of LH pine needles. The sample was collected three times, and 100 mL of each water sample was taken.

The basic test results showed that, when counting number of samples that meets the standard in Table 2, 80% of outflows met the emission standard of GB18918-2002 after adsorption. The adsorption efficiency of phosphorus is approximately 62% in five kinds of water, of which the quality of the second effluent from the southern wastewater treatment plant was the best. The primary test results are shown in Table 3.

**Table 3.** Removal of phosphate in reclaimed water of sewage plant using LH pine needles.

Site	Sample ID	Reclaimed Water	After Adsorption
		P (mg/L)	P (mg/L)
Second class-Western suburb (SW)	1	2.225	1.335
	2	2.072	1.243
	3	2.331	1.362
Second class-Northern suburb (SN)	1	1.835	1.101
	2	2.195	1.318
	3	2.374	1.462
Reclaimed water-Northern suburb (RN)	1	1.113	0.668
	2	1.196	0.717
	3	1.135	0.681
Second class-Southern suburb (SS)	1	0.079	0.049
	2	0.141	0.083
	3	0.061	0.036
Reclaimed water-Southern suburb (RS)	1	0.389	0.232
	2	0.331	0.199
	3	0.391	0.234

Figure 3 shows the impact of LH pine needles adsorbing P in actual wastewater. The efficiency of adsorbing P could be 41–43% at 25 °C. In a broad pH, LH pine needles adsorption to P had a high efficiency, and in the low pH, the adsorption became stronger.

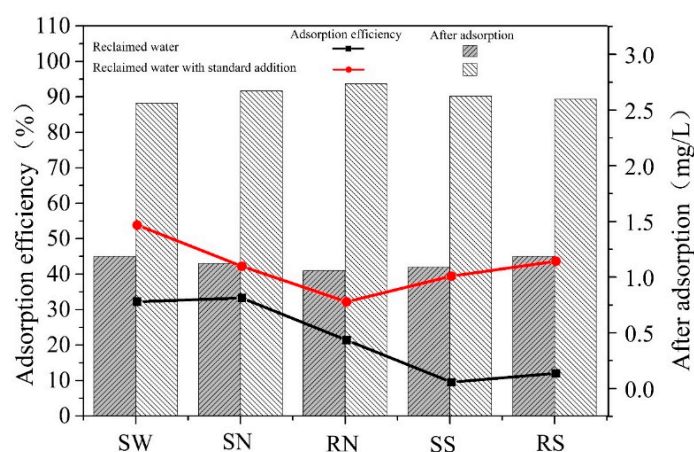


**Figure 3.** Adsorption of phosphorus in LH pine needles in typical sewage treatment plant in Changchun City.

The whole adsorption efficiency was 88–93%, this is consistent with that found in synthetic wastewater. The effects of standard addition were better than that without standard addition. Further, the components in the raw water were complicated—there are many kinds of interfering ions. When  $\text{PO}_4^{3-}$  was at a low concentration, it was disadvantageous to occupy the active position. The concentration of phosphate increases after the addition of the standard, and with the free diffusion effect, the efficiency of LH pine needles clearly increased.

### 3.3. The Analysis of the Recycling Efficiency of LH Pine Needles

In order to enhance the using efficiency of the adsorbent and decrease the production cost, reclaimed saturation LH pine needles have been studied.

Taking into consideration the characteristics of raw needle adsorbent, modified LH pine needles, melting point, thermostability, vapour pressure, as well as physical and chemical characteristics, chemical solvent reclamation was chosen to reclaim the LH pine needles.

In our previous studies, LH pine needles had a better performance in acidic conditions than that in neutral or alkaline conditions. Lewis plays a main role in the adsorbing process under the alkaline condition in which the ligand changing function is inactive. The alkaline eluent was used to avoid decreasing the loading  $La$  when reclaiming the saturated LH pine needles. The elution rate of phosphate was calculated according to the ratio of phosphate in the eluent as Equation (3):

$$E = \frac{C_e \times V}{q_e \times m} \times 100\% \quad (3)$$

where  $C_e$  (mg/L) is the concentration of phosphate in the eluent after equilibrium,  $q_e$  (mg/g) is the adsorbing capacity after equilibrium,  $V$  (mL) is the volume of the eluent and  $m$  (g) is the amount of the LH pine needles.

The elution rate of phosphate in LH pine needles under different eluents is displayed in Table 4.

**Table 4.** Elution rate of phosphate in regeneration solvent.

Regeneration Solvent	NH <sub>3</sub> ·H <sub>2</sub> O	NaCl	NaOH
Elution rate (%)	63	59	91

The regeneration results show that NH<sub>3</sub>·H<sub>2</sub>O, NaCl, and NaOH all had an acceptable performance ( $\geq 59\%$ ) in eluting phosphate on the LH pine needles, signifying it is good for reclaiming LH pine needles under the alkaline condition. The elution rate of NaCl was lower than that of NaOH, which potentially results from the accelerating adsorption process by Cl<sup>−</sup>.

It is suitable for bidentate phosphate to transfer into monodentate under high pH. Accordingly, NaOH elution was chosen as the regeneration solvent. After some cycling, the reclaimed LH adsorbent also had a good performance for phosphate adsorbing.

Regenerating LH pine needle is the reverse reaction process of adsorbing by decreasing the adhesive force. The regeneration formula is presented in Equation (4):

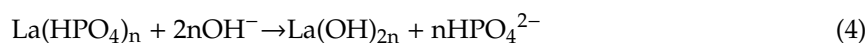
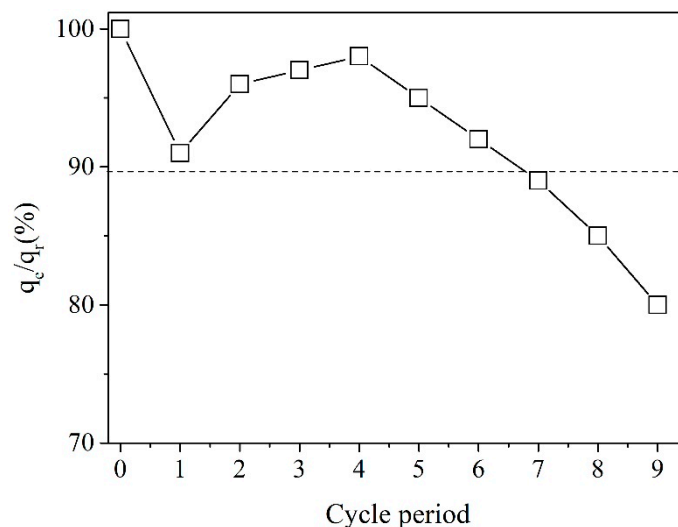


Figure 4 shows the influence of cycling on the adsorption capacity of the reclaimed LH pine needles. Using a 0.1 mol/L NaOH (pH = 10.5) solution, the saturated LH pine needles were eluted 10 times. During the first time, the adsorption capacity of reclaimed LH pine needles could be recovered as much as 90% as the raw LH pine needles. After 2–5 cycles, the adsorption capacity of reclaimed LH pine needles could be recovered higher than 90%.



**Figure 4.** Effect of regenerated LH pine needle use cycle on adsorption capacity.

After 10 times, the adsorption capacity of reclaimed LH pine needles could be recovered as much as 80% of the raw. This result indicates that LH pine needles have a good ability to regenerate.

### 3.4. The Analysis for LH Pine Needles Adsorbing Phosphate Mechanism

Electrostatic force and ligand exchange are most common during adsorption [30]. Some anions—such as  $\text{PO}_4^{3-}$ ,  $\text{NO}_3^-$  and  $\text{AsO}_2^-$  are adsorbed and affected by several factors. However, it is difficult to locate a reasonable adsorption mechanism, as well as the complex system of variable anion concentrations and pH in natural waters [31]. pH plays an important role in the adsorbing process because  $\text{PO}_4^{3-}$  is exchanged with the OH ligand of the adsorbance. At the end of the adsorption, the solution pH decrease may result from the deprotonation of the La active cite ( $\text{La-OH}_2^+ \leftrightarrow \text{La-OH} + \text{H}^+$ ). This result indicates that the main process for  $\text{PO}_4^{3-}$  adsorption was electrostatic attraction.

FT-IR spectra study of the adsorption process often appears the presence of several kinds of structural OH groups. In the FT-IR spectra, the main characteristic peak at  $3445\text{ cm}^{-1}$  in Figure 5 could be attributed to  $-\text{OH}$  from the adsorbed  $\text{H}_2\text{O}$  [32]. The peak at  $814\text{ cm}^{-1}$  could be attributed to  $-\text{CH}$  in aromatic ring structure [33]. The peak at  $2920\text{ cm}^{-1}$  is attributed to  $-\text{CH}_2-$  from the biopolymer, the peak at  $1617\text{ cm}^{-1}$  was attributed to  $\text{C}=\text{O}$  and  $\text{C}=\text{C}$ . The peak at  $1262\text{ cm}^{-1}$  was attributed to  $\text{C}-\text{O}$  from aromatics and  $-\text{OH}$  from phenols, while the peaks at  $672\text{ cm}^{-1}$  and  $524\text{ cm}^{-1}$  are attributed to  $\text{La-OH}$  in  $\text{La}(\text{OH})_3$  [34]. The peak at  $1417\text{ cm}^{-1}$  is attributed to  $\text{NO}_3^-$  from the compound  $\text{La}(\text{NO}_3)_3 \cdot 6\text{H}_2\text{O}$ . After adsorbing, there was a new peak present at  $1060\text{ cm}^{-1}$ , which could be attributed to  $\text{PO}_4^{3-}$  [35,36]. The peak attributed to  $\text{La-O}$  moved from  $524\text{ cm}^{-1}$  to  $571\text{ cm}^{-1}$ . There was a new peak at  $484\text{ cm}^{-1}$ , which could be attributed to  $\text{O-P-O}$  [36]. The essence of these changes is that the metal activity points of lanthanum are occupied by phosphate.

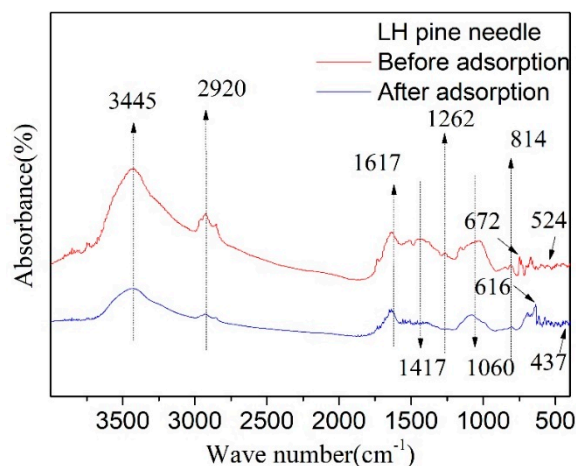


Figure 5. FT-IR atlas of LH pine needles before and after adsorption.

Figure 6 shows the effect of initial-final pH value (3–11) on phosphate adsorption capacity. The point of zero charge ( $pH_{pzc}$ ) of pine needles is approximately 8. Owing to the fact that pH affected the electric charge in the solution and LH pine needles and therefore affected the ions interaction, the adsorbing capacity changed significantly with the changing of pH.

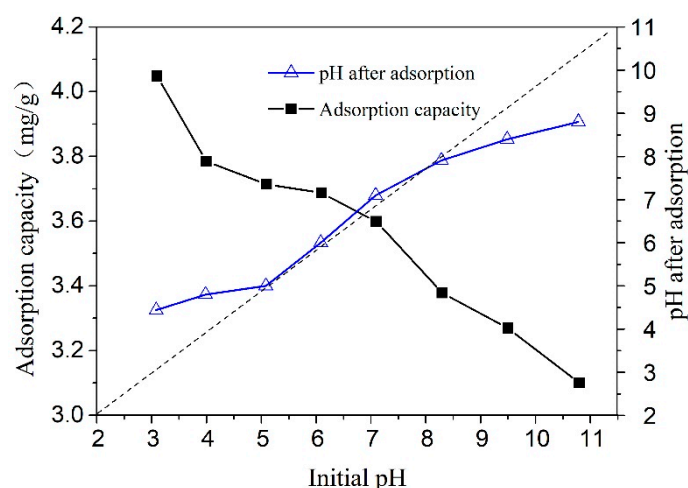


Figure 6. Effect of initial-final pH value on phosphate adsorption capacity.

When pH of solution was higher than  $pH_{pzc}$  of pine needles, there was some negative charge on the surface of pine needles. While the pH of solution was lower than  $pH_{pzc}$  of pine needles, there was some positive charge on the surface of pine needles. The adsorbing capacity to  $PO_4^{3-}$  of LH pine needles changed a lot in the whole range of pH. LH pine needles had the highest adsorption of 5.49 mg/g at  $pH = 3$ . Other pH levels decreased the adsorption for  $PO_4^{3-}$ . When the pH was about 8 ( $pH_{pzc} = 8$ ), the adsorption increased a little and then decreased significantly. In specific, the adsorption decreased by 19.2% at  $pH = 9.6$ .

It could be divided into three stages: I, II and III.

At stage I (pH from 3 to 8), a positive correlation of pH ( $\Delta pH = pH_{initial} - pH_{end}$ ) showed that the adsorption of LH pine needles was a ligand exchange reaction. In fact,  $-OH_2^+$  could occupy the metal binding position more easily than  $-OH$ . When the solution pH was less than  $pH_{pzc}$ , the  $-OH$  on the surface of LH pine needles would be protonized:  $La-OH + H^+ \leftrightarrow La-OH_2^+$ . The positive charge on the surface attracted  $PO_4^{3-}$  by electrostatic force. In the surface of metal oxide, the metal ion had less ligancy, thus, the surface of dried metal oxide showed Lewis acid position.

The metal ion on the surface was first coordinated with the water molecule. Figure 7 shows a La-O ligand bond that was formed by the active position of La and negative oxygen ion of  $\text{PO}_4^{3-}$  under Lewis acid affection.

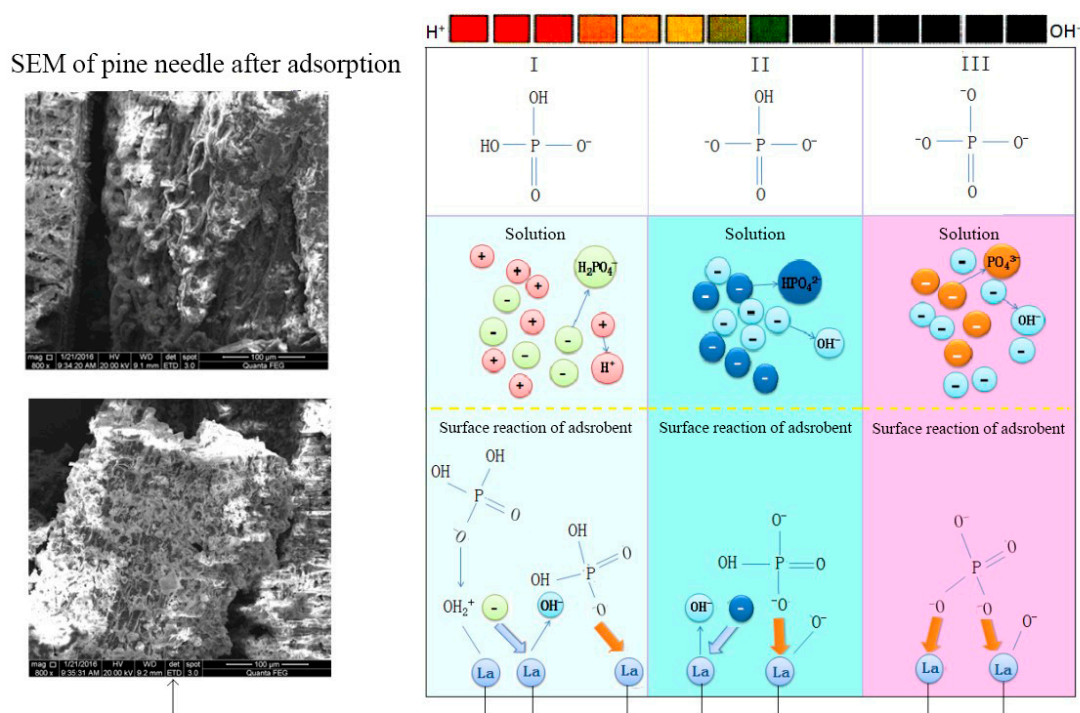


Figure 7. SEM chart and phosphorus adsorption mechanism of LH pine needles.

At stage II ( $8 < \text{pH} < 10$ ), phosphonium ions existed in the form of  $\text{HPO}_4^{2-}$ . Protonation of  $\equiv\text{La-OH}$  became weaker when the pH was less than 10 [37]. In this case, the adsorption of phosphonium ions by the electromagnetic force in the solution is not the main way for it to decrease. Meanwhile, the negative  $\text{La-O}^-$  and  $\text{HPO}_4^{2-}$  had a strong electrostatic repulsion, stopping  $\text{HPO}_4^{2-}$  from approaching the surface of LH pine needles. The mechanism of ligand exchange is that the protonation of LH pine needles surface became weak, resulting in  $\Delta\text{pH}$  decreasing. The increasing of Lewis acid function resulted in negative oxygen of  $\text{HPO}_4^{2-}$  increasing.

At stage III ( $\text{pH} > 10$ ), the adsorption dramatically decreased. The electrostatic repulsion of adsorbent lead ligand exchange reaction was disappearing. Lewis acid reaction controlled the adsorption process.

Figure 7 shows the adsorption to  $\text{PO}_4^{3-}$  mechanism of LH pine needles. Ligand exchange reaction, electrostatic reaction and Lewis acid reaction were  $\text{PO}_4^{3-}$  adsorption mechanism.

Within the entire adsorption process, Ligand exchange reaction and electrostatic reaction became weak with the increase in pH, decreasing adsorption. However, when Lewis acid increased, the adsorption also increased. The SEM analysis of LH pine needles after adsorption shows that there were regular vertical and horizontal textures on the surface and honeycomb cavity within the texture. Alkali alcohol could change the hydrogen bond of woodiness, carbohydrate and cellulose molecule, leading to a fluffy structure [38]. A significant amount of fluffy structure could facilitate LH pine needles adsorbing a certain amount of contaminants, causing a lot of honeycomb cavities being occupied by contaminants.

#### 4. Conclusions

The role of removal P by adsorbent is known to be influenced by many factors. In this study, the influence of pH, concentration and Regenerable was studied. In that wide-area pH range, LH pine has an effective adsorption capacity for phosphorus, and has a strong adsorption effect in the low pH range.

The adsorption of LH on phosphorus in the pH range of 3~11 is divided into three stages. The three main mechanisms of phosphorus adsorption are ligand exchange reaction, electrostatic interaction force and Lewis acid-base interaction.

The results show that at 25 °C, LH pine needle has an effective adsorption capacity for phosphorus of wide-area pH range in reclaimed water, and the adsorption effect is stronger in the low pH range. The highest adsorption efficiency can be achieved 92%, and the treatment capacity of low concentration raw water was also 41%. LH pine needles retain the characteristics of the original amorphous solid, which indicates the structural stability of the modified pine needle. The experimental study on recycling and reuse of LH pine needle showed that LH pine needle had good regeneration performance.

**Author Contributions:** Conceptualization, J.W.; Methodology, C.W. and Z.Y.; Software, Z.Y.; Validation, M.H. and W.Y.; Formal Analysis, C.-H.L.; Investigation, J.W. and X.L.; Data Curation, X.W.; Writing-Review & Editing, X.W. and J.W.

**Funding:** The authors wish to thank the National Natural Science Foundation of China (51708094 and 51808103) and the Science and Technology Development Project of Jilin Province (20180520167JH).

**Conflicts of Interest:** There is no conflict of interest.

## References

1. UNEP. *Wastewater is an Underestimated Resource We Should Not Squander, New UIN Study*; UNEP: Nairobi, Kenya, 2015.
2. Yi, L.L.; Jiao, W.T.; Chen, X.N.; Chen, W.P. An overview of reclaimed water reuse in China. *J. Environ. Sci.* **2011**, *23*, 1585–1593. [[CrossRef](#)]
3. US EPA. *Water Reuse: Trends in the U.S.*; US Environmental Protection Agency: Washington, DC, USA; US Agency for International Development: Washington, DC, USA, 2016.
4. UNESCO. *Wastewater: The Untapped Resource. The United Nations World Water Development Report 2017*; UNESCO: London, UK, 2017.
5. Li, X.; Hu, H.Y.; Yang, J.; Bai, Y. Method to establish the nitrogen and phosphorus standard of reclaimed water reused in landscape. *Ecol. Environ. Sci.* **2009**, *18*, 2404–2408.
6. Shan, B.Q.; Ao, L.; Hu, C.M.; Song, J.Y. Effectiveness of vegetation on phosphorus removal from reclaimed water by a subsurface flow wetland in a coastal area. *J. Environ. Sci.* **2011**, *23*, 1594–1599. [[CrossRef](#)]
7. Gan, W.; Zeng, T.R. A Review of Water Reclamation Research in China Urban Landscape Design and Planning Practice. *J. Phys. Conf. Ser.* **2018**, *989*, 012006. [[CrossRef](#)]
8. Pan, W.Y.; Huang, Q.Z.; Huang, G.H. Nitrogen and Organics Removal during Riverbank Filtration along a Reclaimed Water Restored River in Beijing, China. *Water* **2018**, *10*, 491. [[CrossRef](#)]
9. Drizo, A.; Comeau, Y.; Forget, C.; Chapuis, R.P. Real-time monitoring system for urban wastewater. In Proceedings of the 2017 IEEE Workshop on Environmental, Energy, and Structural Monitoring Systems, Milan, Italy, 24–25 July 2017; pp. 36–40.
10. Drizo, A.; Comeau, Y.; Forget, C.; Chapuis, R.P. Phosphorus saturation potential: A parameter for estimating the longevity of constructed wetland systems. *Environ. Sci. Technol.* **2002**, *36*, 4642–4648. [[CrossRef](#)] [[PubMed](#)]
11. Wang, X.Z.; Liu, Z.M.; Liu, J.C.; Huo, M.X.; Huo, H.L.; Yang, W. Removing phosphorus from aqueous solutions using lanthanum modified pine needles. *PLoS ONE* **2015**, *10*. [[CrossRef](#)] [[PubMed](#)]
12. Xiao, Y.; Li, Y.K.; Ning, Z.G.; Li, P.X.; Yang, P.L.; Liu, C.C.; Liu, Z.W.; Xu, F.P.; Hynds, P.D. Organic contaminant removal efficiency of sodium bentonite/clay (BC) mixtures in high permeability regions utilizing reclaimed wastewater: A meso-scale study. *J. Contam. Hydrol.* **2018**, *210*, 1–14. [[CrossRef](#)] [[PubMed](#)]
13. Pitakteeratham, N.; Hafuka, A.; Satoh, H.; Watanabe, Y. High efficiency removal of phosphate from water by zirconium sulfate-surfactant micelle mesostructure immobilized on polymer matrix. *Water Res.* **2013**, *47*, 3583–3590. [[CrossRef](#)]
14. Barbera, A.C.; Cirelli, G.L.; Cavallaro, V.; Di Silvestro, I.; Pacifici, P.; Castiglione, V.; Toscano, A.; Milani, M. Growth and biomass production of different plant species in two different constructed wetland systems in Sicily. *Desalination* **2009**, *246*, 129–136. [[CrossRef](#)]

15. Nir, O.; Sengpiel, R.; Wessling, M. Closing the cycle: Phosphorus removal and recovery from diluted effluents using acid resistive membranes. *Chem. Eng. J.* **2018**, *346*, 640–648. [[CrossRef](#)]
16. Lima, E.C. Removal of emerging contaminants from the environment by adsorption. *Ecotoxicol. Environ. Saf.* **2018**, *150*, 1–17.
17. Rashed, M.N. Adsorption technique for the removal of organic pollutants from water and wastewater. In *Organic Pollutants-Monitoring, Risk and Treatment*; IntechOpen: Rijeka, Croatia, 2013; pp. 167–194.
18. Xi, Z.M.; Chen, B.L. Removal of polycyclic aromatic hydrocarbons from aqueous solution by raw and modified plant residue materials as biosorbents. *J. Environ. Sci.* **2014**, *26*, 737–748. [[CrossRef](#)]
19. Steinmeier, H. 3. Acetate Manufacturing, Process and Technology 3.1 Chemistry of Cellulose Acetylation. In *Macromolecular Symposia*; Wiley Online Library: Hoboken, NJ, USA, 2004.
20. Teli, M.D.; Valia, S.P. Acetylation of banana fibre to improve oil absorbency. *Carbohydr. Polym.* **2013**, *92*, 328–333. [[CrossRef](#)] [[PubMed](#)]
21. Sun, X.F.; Sun, R.C.; Sun, J.X. Acetylation of sugarcane bagasse using NBS as a catalyst under mild reaction conditions for the production of oil sorption-active materials. *Bioresour. Technol.* **2004**, *95*, 343–350. [[CrossRef](#)]
22. Hussein, M.; Amer, A.A.; El-Maghraby, A.; Hamedallah, N. A comprehensive characterization of corn stalk and study of carbonized corn stalk in dye and gas oil sorption. *J. Anal. Appl. Pyrolysis* **2009**, *86*, 360–363. [[CrossRef](#)]
23. Safarik, I.; Safarikova, M. Magnetic fluid modified peanut husks as an adsorbent for organic dyes removal. In Proceedings of the 12th International Conference on Magnetic Fluids (ICMF12), Sendai, Japan, 1–5 August 2010.
24. Wasay, S.A.; Haron, M.J.; Tokunaga, S. Adsorption of fluoride, phosphate, and arsenate ions on lanthanum-impregnated silica gel. *Water Environ. Res.* **1996**, *68*, 295–300. [[CrossRef](#)]
25. Biswas, B.K.; Inoue, K.; Ghimire, K.N.; Ohta, S.; Harada, H.; Ohto, K.; Kawakita, H. 2007 The adsorption of phosphate from an aquatic environment using metal-loaded orange waste. *J. Colloid Interface Sci.* **2007**, *312*, 214–223. [[CrossRef](#)]
26. Benyoucef, S.; Amrani, M. Removal of phosphorus from aqueous solutions using chemically modified sawdust of Aleppo pine (*Pinus halepensis* Miller): Kinetics and isotherm studies. *Environmentalist* **2017**, *31*, 200–207. [[CrossRef](#)]
27. Zhang, J.D.; Shen, Z.M.; Shan, W.P.; Mei, Z.J.; Wang, W.H. Adsorption behavior of phosphate on lanthanum (III)-coordinated diamino-functionalized 3D hybrid mesoporous silicates material. *J. Hazard. Mater.* **2011**, *186*, 76–83. [[CrossRef](#)]
28. Keiluweit, M.; Nico, P.S.; Johnson, M.G.; Kleber, M. Dynamic molecular structure of plant biomass-derived black carbon (Biochar). *Environ. Sci. Technol.* **2010**, *44*, 1247–1253. [[CrossRef](#)] [[PubMed](#)]
29. De Lima, A.C.A.; Nascimento, R.F.; de Sousa, F.F.; Filho, J.M.; Oliveira, A.C. Modified coconut shell fibers: A green and economical sorbent for the removal of anions from aqueous solutions. *Chem. Eng. J.* **2012**, *185*, 274–284. [[CrossRef](#)]
30. Tamijani, A.A.; Salam, A.; de Lara-Castells, M.P. Adsorption of noble-gas atoms on the TiO<sub>2</sub> (110) surface: An Ab initio-assisted study with van der Waals-corrected DFT. *J. Phys. Chem. C* **2016**, *120*, 18126–18139. [[CrossRef](#)]
31. Corum, K.; Abbaspour Tamijani, A.; Mason, S. Density functional theory study of arsenate adsorption onto alumina surfaces. *Minerals* **2018**, *8*, 91. [[CrossRef](#)]
32. Chen, B.L.; Johnson, E.J.; Chefetz, B.; Zhu, L.Z.; Xing, B.S. Sorption of polar and nonpolar aromatic organic contaminants by plant cuticular materials: Role of polarity and accessibility. *Environ. Sci. Technol.* **2005**, *39*, 6138–6146. [[CrossRef](#)] [[PubMed](#)]
33. Chen, B.L.; Zhou, D.D.; Zhu, L.Z. Transitional adsorption and partition of nonpolar and polar aromatic contaminants by biochars of pine needles with different pyrolytic temperatures. *Environ. Sci. Technol.* **2008**, *42*, 5137–5143. [[CrossRef](#)] [[PubMed](#)]
34. Chun, Y.; Sheng, G.Y.; Chiou, C.T.; Xing, B.S. Compositions and sorptive properties of crop residue-derived chars. *Environ. Sci. Technol.* **2004**, *38*, 4649–4655. [[CrossRef](#)] [[PubMed](#)]
35. Li, H.; Ru, J.Y.; Yin, W.; Liu, X.H.; Wang, J.Q.; Zhang, W.D. Removal of phosphate from polluted water by lanthanum doped vesuvianite. *J. Hazard. Mater.* **2009**, *168*, 326–330. [[CrossRef](#)]

36. Li, L.; Jiang, W.G.; Pan, H.H.; Xu, X.R.; Tang, Y.X.; Ming, J.Z.; Xu, Z.D.; Tang, R.K. Improved luminescence of lanthanide (III)-doped nanophosphors by linear aggregation. *J. Phys. Chem. C* **2007**, *111*, 4111–4115. [[CrossRef](#)]
37. Huang, X.; Foster, G.D.; Honeychuck, R.V.; Schreifels, J.A. The maximum of phosphate adsorption at pH 4.0: Why it appears on aluminum oxides but not on iron oxides. *Langmuir* **2009**, *25*, 4450–4461. [[CrossRef](#)]
38. Chen, G.Y.; Zheng, Z.; Luo, Y.; Zou, X.X.; Fang, C.X. Effect of alkaline treatment on anaerobic digestion of rice straw. *Huanjing Kexue Environ. Sci.* **2010**, *31*, 2208–2213.



© 2019 by the authors. Licensee MDPI, Basel, Switzerland. This article is an open access article distributed under the terms and conditions of the Creative Commons Attribution (CC BY) license (<http://creativecommons.org/licenses/by/4.0/>).